



Annese, V. F., Hu, C., Barrett, M. P., Jones, R. and Cumming, D. R. S. (2022) A CMOS-based multi-omics detection platform for simultaneous quantification of proteolytically active prostate specific antigen and glutamate in urine. *IEEE Sensors Journal*, 22(19), pp. 18870-18877.



Copyright © 2022 IEEE. Reproduced under a [Creative Commons Attribution 4.0 International License](https://creativecommons.org/licenses/by/4.0/).

For the purpose of open access, the author(s) has applied a Creative Commons Attribution license to any Accepted Manuscript version arising.

<https://eprints.gla.ac.uk/276525/>

Deposited on: 8 August 2022

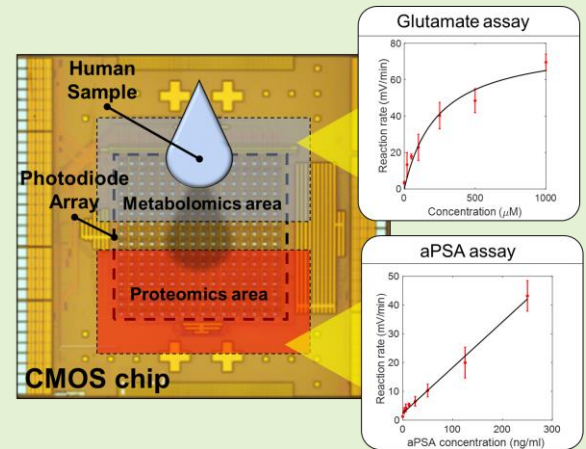
Enlighten – Research publications by members of the University of Glasgow
<https://eprints.gla.ac.uk>

A CMOS-Based Multi-Omics Detection Platform for Simultaneous Quantification of Proteolytically Active Prostate Specific Antigen and Glutamate in Urine

V. F. Annese, C. Hu, M.P. Barrett, R. Jones, David R.S. Cumming

Abstract— By combining information such as genomics, proteomics, and metabolomics data, multi-omics methodologies have the potential to reveal the otherwise invisible processes of carcinogenesis. Using these data, a new generation point-of-care (POC) devices may support patient care through rapid diagnosis involving accurate and simultaneous multi-omics measurements. In this work we present a proof-of-concept portable system capable of measuring a metabolite (glutamate) and a protein (proteolytically active prostate-specific antigen - aPSA) simultaneously on single device in a two-minute interval using on-chip optical methods. The device has the potential to improve the current diagnostic pathways of prostate cancer by reducing the high false-positive rate with the widely used total prostate-specific antigen and aPSA in buffer and synthetic urine. For the glutamate assay, the limit of detection (LOD) and resolution were found to be $0.9 \mu\text{M}$ and $2.7 \mu\text{M}$. LOD and resolution for aPSA were 0.5 ng/ml and 2.0 ng/ml . The LOD and resolution achieved using this device are therefore in line with human physiological ranges. The platform is suitable for accommodating two independent optical assays therefore chemistry can be modified to measure different analytes regardless of their nature. This technological breakthrough has the potential to deliver an accurate multi-omics portable device for prostate cancer and may be extended to other diseases.

Index Terms— Multi-omics; Omics; Cancer; CMOS; Point-of-care; Mobile technology; Lab-on-chip; Microfabrication; Microarrays; Sensor array.



I. INTRODUCTION

Many disease states are characterized by deviations in abundance of biomolecules which can be used in diagnosis. These biomolecules include nucleic acids, proteins, and metabolites. The chemistry required to quantify each of these molecular types is different hence most diagnostic devices investigate only a single class of biomarker. However, multi-

omic approaches to measure different classes of biomarker simultaneously has the potential to provide combined diagnostic information to improve the sensitivity and specificity of diagnostic testing.

V.F.A., C.H., D.R.S.C. are with the James Watt School of Engineering, University of Glasgow, Glasgow, G12 8QQ, UK (e-mail: david.cumming.2@glasgow.ac.uk). M.P.B. is with Institute of Infection, Immunity and Inflammation, University of Glasgow, Glasgow, G12 8TA, UK and Glasgow Polyomics, College of Medical, Veterinary and Life Sciences, University of Glasgow, Glasgow, G61 1BD, UK. R.J. is with Institute of Cancer Sciences, University of Glasgow, Beatson West of Scotland Cancer Centre, Glasgow, G12 0YN, UK. Corresponding author. E-mail: david.cumming.2@glasgow.ac.

Multi-omics strategies show promise to untangle the complicated pathways of carcinogenesis by combining multi-level omics approaches, including genomics, proteomics, and metabolomics [1][2]. Multi-omics diagnostics can be particularly beneficial for prostate cancer (PCa) where the current clinical standard blood test, total prostate specific antigen (tPSA), is notoriously unreliable [3]. PCa is the most common cancer in developed countries in men, claiming more than 300,000 lives each year. Typically, an elevated tPSA result triggers a sequence of invasive testing including digital rectal examination, multiparametric magnetic resonance imaging and biopsy, leading to a diagnosis [4]. The high false-positive rate of tPSA (~70%) results in many unnecessary

invasive tests which are expensive and detrimental to the mental and physical health of patients. Therefore, new, cost-effective tools measuring single or multiple biomarkers of different omics classes are needed to improve the diagnostic path.

Among protein biomarkers for PCa, PSA isoforms are candidate tools to improve PCa diagnostic accuracy [5]. PSA isoforms are typically divided into enzymatically active and inactive forms [6, 7]. Proteolytically active PSA (aPSA), mainly found in prostatic fluids and urine has been shown to be a valid candidate to improve the diagnostic accuracy for prostate cancer when used together with a standard blood tPSA [8, 9]. However, current antibody-based strategies for measuring tPSA such as fluorescent, absorption and electrochemical immunoassays require several wash steps and cannot discriminate between active and inactive PSA.

Several metabolites in body fluids including blood and urine have also been suggested as potential biomarkers for PCa [10]. The altered metabolism of cancer cells produces substantial and detectable modifications in the entire human metabolome [11, 12]. Glutamate has drawn particular attention as it directly correlates with the energy cycle of cancer cells [13]. A correlation between urinary glutamate and PCa aggressiveness (Gleason score) has also been presented [14].

As cancer research enters the multi-omics era [15], technology also needs to evolve. Accurate and cost-effective point-of-care (POC) technology has been developed to deliver rapid measurement of multiple biomarkers in readily available body fluids for different omics types, including genomics, proteomics and metabolomics [10, 16, 17, 18]. POC technologies typically target only one omics type as different omics usually require different chemistries, processing, and equipment [19]. Since the construction of a single multi-omics POC platform is challenging, current multi-omics studies use artificial intelligence algorithms to combine data from different pieces of laboratory equipment [3]. However, this approach limits the use of multi-omics to laboratory testing and does not herald a future POC capability.

The use of CMOS-based technology to measure multiple metabolites has previously been demonstrated [10, 20, 21] but the possibility of measuring proteins and metabolites at the same time has not previously been studied. As a proof-of-concept aPSA and glutamate were measured in urine as a diagnostic for PCa, the relevance of which has been shown [8, 9, 14]. The multi-omics platform used in this work has a 16x16 array of photodiodes fabricated using complementary metal oxide semiconductor (CMOS) technology. Two microwells were fabricated on top of the sensing area to create two separate reaction zones. The microwells were used simultaneously to quantify glutamate using a wash-less enzymatic colorimetric assay and aPSA using a chromogenic assay. We demonstrate that the multi-omics device can measure glutamate and aPSA in urine in two minutes with limits of detection (LOD) of 0.9 μM and 0.5 ng/ml respectively. This new technology has the potential to deliver an accurate multi-omics portable device with implications extending beyond the immediate clinical test case of PCa.

II. MATERIALS AND METHODS

A. Sensing Platform

A 16x16 array of photodiodes was designed and fabricated using a commercially available CMOS 350 nm high voltage 4-metal process provided by austriamicrosystems (AMS). Each pixel of the array integrates a photodiode that is 100 x 100 μm in size, leading to a total sensitive area of 1.6 x 1.6 mm. The size of the entire CMOS chip is 3.4 x 3.6 mm. The sensitive area of the sensor array was divided into two independent regions accommodating a glutamate colorimetric assay and an aPSA chromogenic assay, as shown in Fig. 1a. The CMOS chip, including the noise level of the platform, has been fully characterized in previous work [20], [21]. Fig. 1b shows the average spectral response of the photodiode array. The responsivity was normalised to its maximum at 575 nm. A second responsivity peak was observed at 620 nm.

To fabricate the two independent reaction zones on the sensing area, the CMOS chip was wire-bonded on to a ceramic 120 pin grid array (PGA) chip package. Two sacrificial polydimethylsiloxane (PDMS) microblocks of 600 μm x 600 μm and height of 1500 μm (SYLGARD 184 Silicone Elastomer Kit, Dow Corning) were temporarily bonded on to the pixel area of the CMOS-chip. A mixture of epoxy and curing agent (100:45 w/w, 302-3M EPO-TEK) was prepared and carefully micropipetted over the area of the CMOS chip and the contact pads. After the epoxy resin was cured at room temperature for 24h, the PDMS microblocks were removed leaving two microwells exposed.

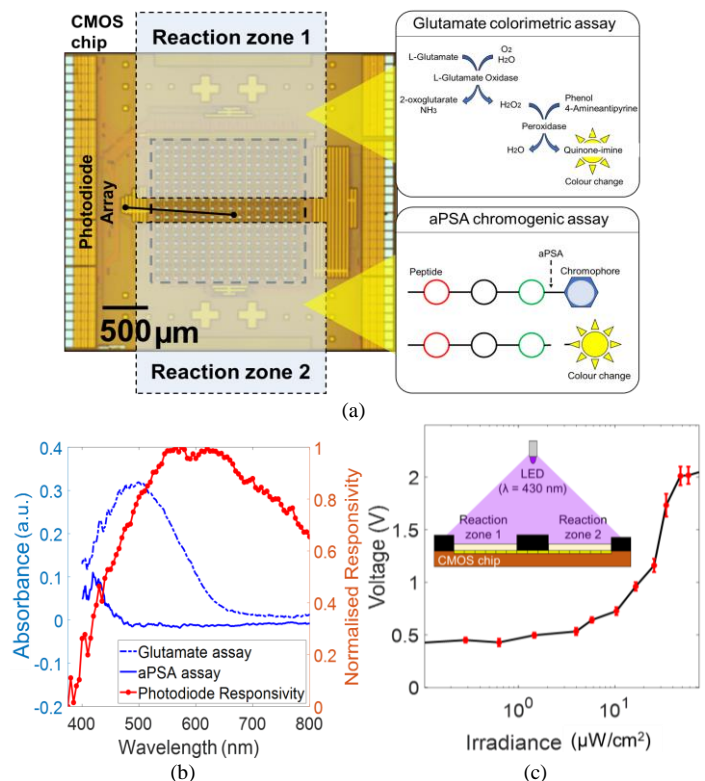


Fig. 1. (a) Architecture and working principle of the device. (b) Normalised responsivity of the photodiode array (red) and absorbance spectra for glutamate (dotted blue) and aPSA (solid blue) assays measured with a spectrophotometer (fftA-1 from Foster and Freeman). (c) Output characteristic of the photodiode array measured at 430 nm. Inset: measurement setup (not in scale).

The epoxy resin also encapsulates the electrical connections of the CMOS chip (left and right pads in Fig. 1a). The top surface of the standard CMOS chip is also protected by a thin polyimide layer [20]. Therefore, the photodiode array can safely operate when the liquid sample is introduced into the microwell.

B. Glutamate Assay

To perform the glutamate test, an enzyme-based colorimetric assay was used. We employed a reagent formulation that uses glutamate oxidase (GLOX E.C.-1.4.3.11) that liberates H_2O_2 during the reaction with glutamate.

The H_2O_2 produced reacts in turn with peroxidase (HRP E.C.-1.11.1.7), phenol and 4-aminoantipyrine (4-AAP) to produce a colorimetric change that increases the optical absorbance of the liquid in the microwell that is in turn detected by the on-chip photodiodes. The initial reaction rate depends on the concentration of the substrate according to Michaelis-Menten model [10]. 100 μ l of reagent solution for glutamate assay was prepared by mixing 33.5 μ l of GLOX (4 U/mL), 33.5 μ l of HRP (150 U/mL), 16.5 μ l of phenol (44.5 mM) and 16.5 μ l of 4AAP (10.5 mM). All reagents were purchased from Sigma Aldrich and freshly prepared in assay buffer (50 mM Tris, 1 M NaCl, pH 8.0). A stock solution of 5 mM L-glutamic acid purchased from Sigma Aldrich in water buffer was also prepared and used to prepare test solutions.

C. aPSA Assay

To perform the aPSA test, a chromogenic assay was used. The synthetic peptide substrate N-Methoxy-Succinyl-L-Arginyl-L-Prolyl-L-Tyrosine-p-Nitroanilide (MeO-Suc-Arg-Pro-Tyr-pNA) was purchased from Cambridge Bioscience. PSA is a chymotrypsin-like serine protease belonging to the human kallikrein family, specifically known as kallikrein-related peptidase 3 (KLK3). In its purified form PSA is an active enzyme that is produced by the prostate gland. PSA isoforms are then generated by a sequence of transformations when PSA reaches the blood stream.

The chromogenic substrate takes advantage of the enzymatic activity of aPSA to cleave the peptide and release free p-nitroanilide (pNA). The release of free pNA modifies the optical absorbance of the solution and can be measured with the photodiode array in the microwell. A reaction solution containing 2 mM MeO-Suc-Arg-Pro-Tyr-pNA was produced according to the manufacturer's guidelines. The peptide was freshly diluted in assay buffer (50 mM Tris, 1 M NaCl, pH 8.0). Recombinant human KLK3 (rhKLK3) was purchased from R&D systems – BioTechne. A stock solution of 12.5 μ g/mL of aPSA was prepared according to the manufacturer guidelines [22] and used to prepare test solutions.

D. Experimental Method

The sensor array was connected to a custom hand-held reader using a zero-insertion force socket. The reader was composed of a custom PCB board and a microcontroller (ST Nucleo F334R8 board) programmed before use with custom firmware. The reader was used to interface the sensor array for addressing, data digitization (12 bits, 3.3V range) and transmission to a personal computer (HP EliteBook i7-8650u 16 GB) via a USB link. The reader was powered by the USB

link (5 V) that in turn powered the sensor array (3.3 V). Data was collected with an average frame per second of 8.3 fps.

To verify that both glutamate and aPSA assays were working as expected, the absorbance spectrum for both the assays was initially assessed using a micro-spectrometer (ffTA-1 from Foster and Freeman). The absorbance spectrum of the glutamate assay was measured by mixing 50 μ l of 0.4 mM L-glutamic acid with 50 μ l of the reagent solution in a 384-well plate. The absorbance spectrum of the aPSA assay was measured by mixing 50 μ l of 800 ng/ml aPSA with 50 μ l of the reaction solution in a 384-well plate. Spectra were measured after a 24h incubation at room temperature. Both the spectra for glutamate and aPSA are shown in Fig. 1b. For glutamate, an absorbance peak was observed at 499 nm and the full width at half maximum (FWHM) of the curve was 160 nm. For a PSA, an absorbance peak was observed at 419 nm and the FWHM of the curve was 34 nm.

For both glutamate and aPSA assays, experiments on-chip were performed in buffer and in synthetic urine. Test solutions were obtained by spiking assay buffer (50 mM Tris, 1 M NaCl, pH 8.0) or synthetic urine (artificial stabilized urine BZ104 from Biochemozone) with a known concentration of glutamate and aPSA stock solutions. The synthetic urine did not contain any glutamate or aPSA prior to being spiked. Additional details regarding the preparation of synthetic urine samples are reported in the Supplementary Material.

For each experiment, 50 μ l of reaction solution and 50 μ l of test solution were introduced into the respective microwell by manual pipetting. No further wash step or incubation was needed. Optical absorbance at 430 nm was measured using the photodiode array for 2 minutes after the reaction was started. Measurements were performed at room temperature. An 8 mW LED ($\lambda=430$ nm, FWHM=20 nm) from Thorlabs was used to illuminate the sensing area of the sensor array. The distance between the LED and the sensor array was 10 cm. No lens was used in this setup. All the measurements were performed in dark conditions. The LED power was adjusted to have the array working in the linear region of the characteristic in Fig. 1c (irradiance value 30 μ W/cm²). The irradiance value was kept constant in all the measurements. The wavelength of 430 nm was selected as a tradeoff between the absorbance peak of the two reactions and the responsivity peak of the photodiode array (Fig. 1b). The output characteristic of the photodiode array at 430 nm was measured and is shown in Fig. 1c. The measurement setup is shown in the inset of Fig. 1c. The CMOS chips employed in this work were all from the same fabrication batch.

The device was cleaned and re-used. A cleaning procedure after every measurement was used to avoid cross-contamination. The cleaning process involved a sequential rinse in DI water, IPA, and then ethanol. The washing sequence was repeated multiple times. Nitrogen was used to blow dry the device after the cleaning procedure.

E. Data Analysis

The measure of the initial reaction rate was performed using a custom Matlab program. Output data from pixel in the same microwell were low pass filtered and averaged. Unresponsive sensors or sensors affected by strong artifacts were excluded

from the averaging process after visual inspection. The use of a sensor array is particularly beneficial to improve the signal-to-noise ratio as shown in previous works [23]. The data was then temporally averaged in non-overlapping 1 second intervals and fitted to the Michaelis-Menten model. The Michaelis-Menten model links the reaction rate to the initial concentration of the substrate and enzymatic activity as follows [24]:

$$\frac{d[P]}{dt} = \frac{V_m \cdot [S]}{K_m + [S]} \quad (1)$$

where [P] and [S] are the concentrations of the reaction product and the substrate, V_m is the maximum rate achieved by the system and K_m is the Michaelis constant. V_m is proportional to the concentration of the enzyme used in the reaction. In the glutamate reaction, glutamate is the substrate. In the aPSA reaction, aPSA is the enzyme and the chromogen is the substrate. In both cases, measuring the initial reaction rate under known conditions of the other reactants enables measurement of the concentrations of glutamate or aPSA.

The initial rate of the reaction was determined by differentiation of the processed data in the first two minutes of the reaction. Experiments in buffer were repeated three times for each data point and results were extracted as average and standard deviation. Experiments in synthetic urine were repeated two times for each data point and results were extracted as average and range of the measurement. Additional details regarding data processing are reported in the Supplementary Material.

III. RESULTS AND DISCUSSION

A. Assay in Buffer

For the glutamate assay, the platform was tested and characterized using buffer solutions with 7 concentrations of glutamate (0 μM , 20 μM , 50 μM , 100 μM , 250 μM , 500 μM and 1 mM). Increasing the concentration of glutamate created a detectable increase in the initial reaction rate (see Fig. 2a). Average reaction rates for each concentration measured in the first 2 minutes of the reaction were used to obtain a calibration curve shown in Fig. 2b.

For the aPSA assay, the platform was tested and characterized using buffer solutions with 8 concentrations of aPSA (0 ng/mL, 3.125 ng/mL, 6.25 ng/mL, 12.5 ng/mL, 25 ng/mL, 50 ng/mL, 125 ng/mL, 250 ng/mL). Similarly, increasing aPSA concentrations created an increase of the reaction rate (see Fig. 2c). The calibration curve of the assay was extracted using the initial rates of the reactions and is shown in Fig. 2d. Relevant metrics for glutamate and aPSA assays in buffer were measured using the respective calibration curve and summarized in Table 1.

For the glutamate assay, LOD and resolution were found to be 0.9 μM and 2.7 μM . Normal urine glutamate concentration is in the range 3.3–18.4 μM per mM of creatinine [25]. Urine creatinine is typically 15.75 mM (\approx 1.78 g/L [26]) yielding a urine glutamate concentration in the range 52 – 290 μM . The scientific literature shows that urine glutamate might be more than doubled in patients with Gleason score 8 or higher with respect to healthy men [14]. Therefore, the LOD and

resolution data obtained in this work are suitable for measuring glutamate in urine. For aPSA assay, LOD and resolution were 0.5 ng/ml and 2.0 ng/ml respectively. A urinary tPSA concentrations < 150 ng/mL in conjunction with elevated serum tPSA concentrations > 4 ng/mL have been linked to prostate cancer diagnosis [27]. In urine, PSA mainly exists in its free form and is enzymatically active [7, 28]. Therefore, the LOD and resolution achieved by this device are in line with blood and urine physiological ranges of aPSA.

B. Simultaneous Assay in Buffer

Experiments were carried out to demonstrate the suitability of the platform for simultaneous assays of glutamate and aPSA in buffer. On the same device, 50 μl of reaction solution for the glutamate assay were introduced into one microwell.

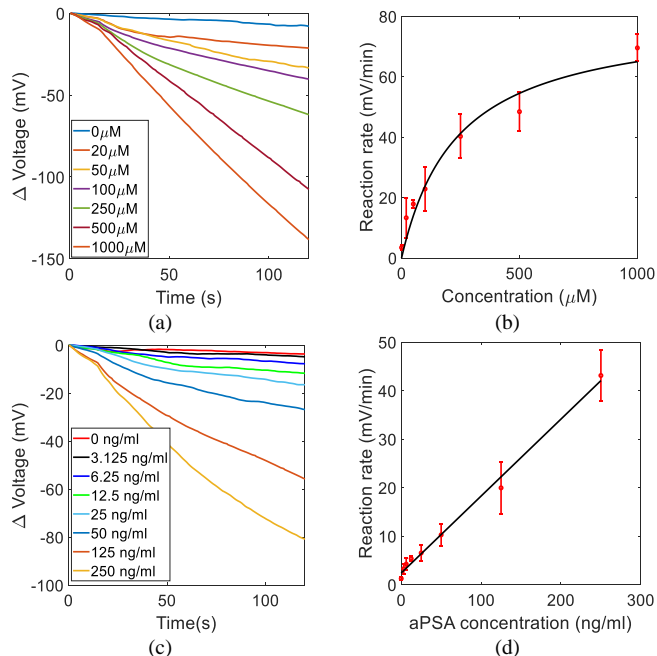


Fig. 2. Assay in buffer. (a) Averaged raw data for different concentrations of glutamate; (b) Calibration curve for glutamate assay in buffer. (c) Averaged raw data for different concentrations of aPSA; (d) Calibration curve for aPSA assay in buffer.

TABLE I.

PLATFORM CHARACTERIZATION FOR GLUTAMATE AND APSA ASSAYS IN BUFFER USING THE PROPOSED PLATFORM

Variable	Glutamate	aPSA
Sample volume	50 μl per μwell	
Total assay volume	100 μl per μwell	
Working wavelength	430 nm	
Test duration	2 min	
Linearity (R^2)	0.97 ⁽⁵⁾	0.99
Precision ⁽¹⁾	20.9 %	22.9 %
Analytical Sensitivity ⁽²⁾	0.3 (mV \cdot min ⁻¹)/ μM	0.16 (mV \cdot min ⁻¹)/(ng/ml)
Resolution ⁽³⁾	2.7 μM	2.0 ng/ml
LOD ⁽⁴⁾	0.9 μM	0.5 ng/ml

⁽¹⁾ measured as the average over the relative standard deviations of the measurements per each concentration. ⁽²⁾ measured as the slope of linearized calibration curve in the initial linear. ⁽³⁾ measured as the ratio between standard deviation of the blank experiments and the analytical sensitivity (IUPAC definition). ⁽⁴⁾ measured as the average plus 3.3 times the standard deviation of the of the blank experiments (IUPAC definition). LOD can be converted to μM using the calibration curve. ⁽⁵⁾ Glutamate linearity was calculated in the range 0 – 250 μM .

50 μl of reaction solution for the aPSA were introduced in the second microwell. Four test solutions with different concentrations of glutamate and aPSA were prepared in buffer. 50 μl of test solution was introduced by pipetting into each microwell, effectively starting the respective reaction. The results of the experiment are illustrated in Fig. 3. The first test solution did not contain any glutamate or aPSA therefore only background signal was observed (Fig. 3a). The microwells used for the glutamate and aPSA assays each provided a clearly detectable signal when a solution containing only glutamate or aPSA was introduced to the device (Fig. 3b, c). To complete the study a solution containing both glutamate and aPSA was introduced to the device. A strong signal was observed from both the microwells (Fig. 3d).

Data was processed and initial reaction rates were measured for each experiment for the first two minutes of the experiment. Reaction rates for the four testing conditions are shown in Fig 3e-h. Measured initial reaction rate from these experiments were similar to those observed in the calibration curves.

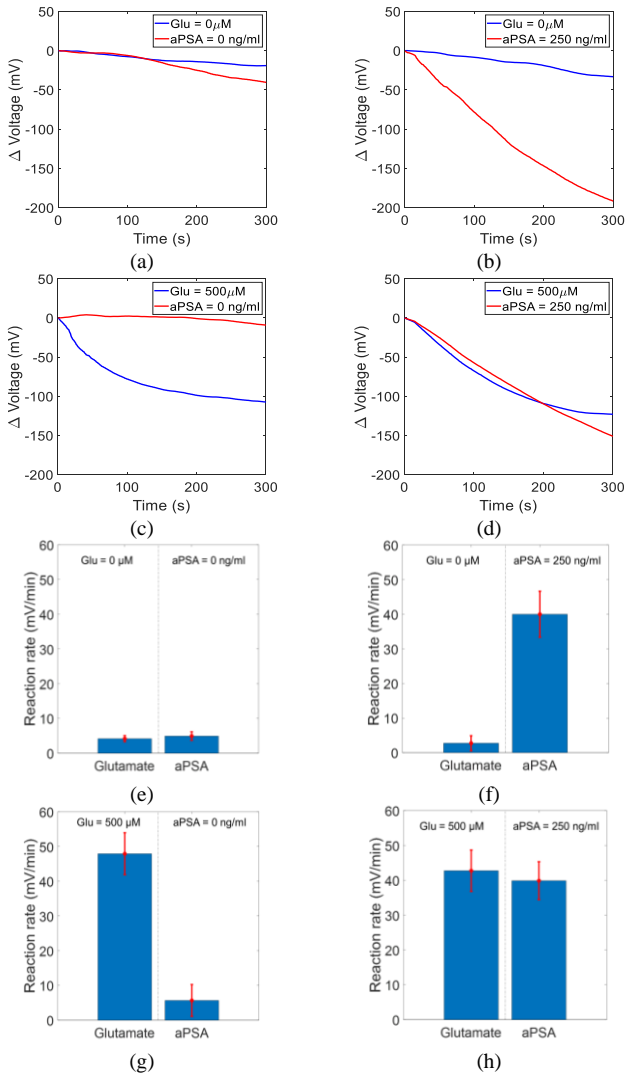


Fig. 3. Simultaneous assays in buffer. (a)-(d) Typical output of the two reaction zones, where one is dedicated to glutamate assay (blue curve) and the other to the aPSA assay (red curve). (e)-(h) Initial reaction rate (2 minutes) in the respective reaction zones.

No obvious crosstalk was observed in the experiments indicating that the glutamate and aPSA were detected independently thus the platform successfully quantifies a metabolite (glutamate) and a protein (aPSA) simultaneously.

C. Simultaneous Assay in Urine

Further validation of the platform for multi-omics testing in synthetic urine was then conducted. Urine was selected as the medium of interest since there is growing interest in improved urine testing for PCa [29]. Urine testing benefits from easy sample collection and elevated concentrations of numerous biomarkers of interest compared to blood. aPSA is predominantly present in urine [7] and urinary glutamate has also been indicated as a promising PCa biomarker [14].

The platform was tested on seven synthetic urine samples. The synthetic urine did not contain any glutamate or aPSA.

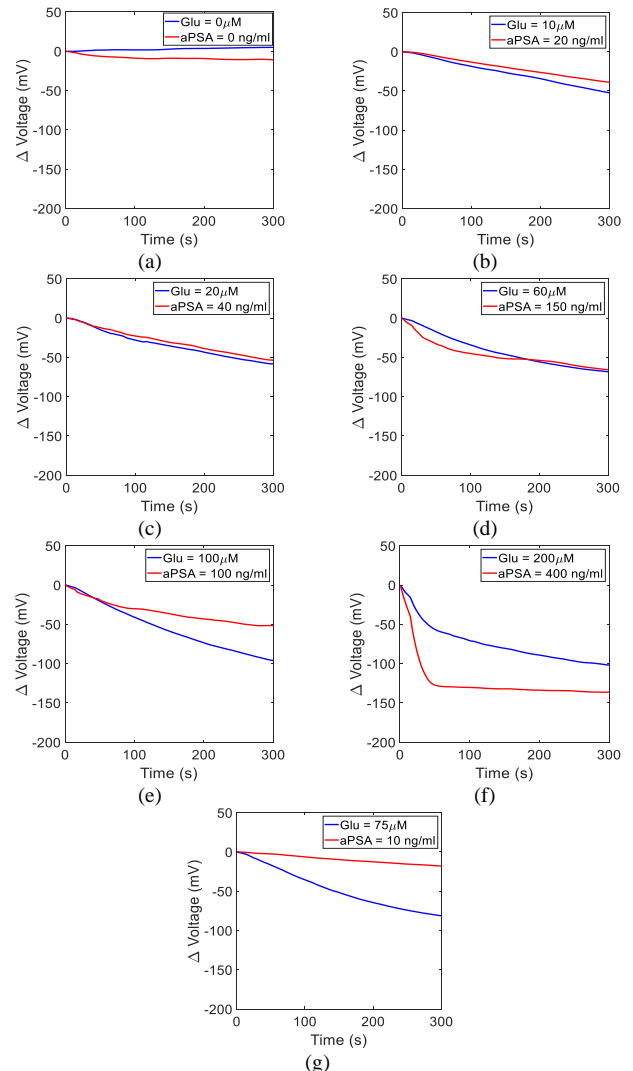


Fig. 4. Simultaneous assay in synthetic urine. Typical output of the two reaction zones for glutamate (blue curve) and aPSA (red curve) assays. Synthetic urine sample was spiked with different concentrations of glutamate and aPSA: (a) Glu = 0 μM , aPSA = 0 ng/ml; (b) Glu = 10 μM , aPSA = 20 ng/ml; (c) Glu = 20 μM , aPSA = 40 ng/ml; (d) Glu = 60 μM , aPSA = 150 ng/ml; (e) Glu = 100 μM , aPSA = 100 ng/ml; (f) Glu = 200 μM , aPSA = 400 ng/ml; (g) Glu = 75 μM , aPSA = 10 ng/ml.

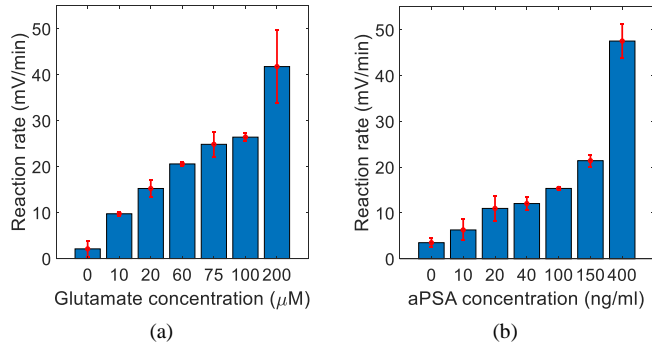


Fig. 5. Initial reaction rate (2 minutes) in the respective reaction zones for (a) glutamate and (b) aPSA in synthetic urine. Concentrations have been sorted in ascending order for each graph. Blue and red bars are respectively average and range of the measurements for each concentration calculated over two samples.

Therefore, test samples were obtained by spiking synthetic urine with known concentrations of glutamate and aPSA. Glutamate and aPSA solutions were prepared as described in the materials and methods section and experiments were conducted using the same procedure outlined for the simultaneous experiments in buffer (Section 3.B).

The concentration of glutamate in the first six test samples was 0 μM , 10 μM , 20 μM , 60 μM , 100 μM and 200 μM . The concentration of aPSA used in the same six test samples was 0 ng/ml, 20 ng/ml, 40 ng/ml, 150 ng/ml, 100 ng/ml and 400 ng/ml, respectively. The test samples were tested in the same order as reported above. To confirm that the sensor was not subject to any form of hysteresis when exposed to high glutamate or aPSA concentrations, a seventh sample with lower concentrations at 75 μM of glutamate and 10 ng/ml aPSA was then tested. The first test sample (0 μM glutamate and 0 ng/ml aPSA) was used as background measurement (Fig. 4a). The other test samples produced clearly detectable signals dependent on the concentrations of glutamate and aPSA (Fig. 4b-g).

For each experiment, the initial rate of reaction was measured using the first 2 minutes of the recordings. The initial reaction rates observed in the simultaneous assays in urine are shown in Fig. 5a-b. In Fig. 5a and Fig. 5b, samples were sorted with the respective concentration of the biomarker in an ascending order. The initial reaction rates measured simultaneously in synthetic urine were comparable to those observed in the buffer calibration curves. This provides a proof of principle that the platform is suitable for quantifying glutamate and aPSA simultaneously in urine.

D. Discussion

We have presented a proof-of-concept that simultaneous measurement of metabolites and proteins is feasible using a multi-omic device with LOD suitable for physiological range measurement. The buffer glutamate assay LOD is comparable to other GLOX-based glutamate sensors which is typically below 1 μM [30]. The buffer aPSA LOD is also similar to the one achieved in similar works [7]. The test time (2 min) and the absence of washing steps or incubation match commercial POC platform requirements [19]. Unlike other state-of-the-art devices, this platform can measure both a metabolite

(glutamate) and a protein (aPSA) simultaneously. This feature is currently missing in state-of-the-art devices.

The use of a CMOS-based photodiode array is particularly advantageous for affordability. If mass produced the device could reach cost levels allowing for single use disposal devices. The use of an optical sensor array with physical separation ensuring low crosstalk is beneficial for scalability. Potentially more microwells could be integrated on the platform, for instance by extending the CMOS sensitive area or further miniaturizing sample application capability. Since the techniques adopted in this work, including CMOS technology, epoxy moulding and bio-specific assays, are suitable for large-scale production we believe that the platform we have demonstrated is not limited to only two analytes; it can be potentially scaled-up to accommodate many optical assays, regardless of their nature.

In this work we have demonstrated the multi-omics capability of a CMOS sensing platform. The platform was tested on urine samples. Since concentrations of aPSA in blood and urine of healthy subjects and men affected by prostate cancer are still under research therefore we have assumed the aPSA concentration to be comparable with the tPSA concentration. We believe that the platform can also be used for multi-omics testing of other body fluids, including blood serum and plasma. For example, plasma aPSA and plasma glutamate have also been linked to PCa [31]. Processing techniques are also available to activate other inactive forms of blood PSA using, for instance, human kallikrein 2 (hK2) [32].

Whilst urinary tests are undoubtedly more convenient than blood tests, they do present challenges associated with wide-ranging physiological variation in water content that will result in a wide reference range of ‘normal’ for any diagnostic urinary analyte. To control for this, the multi-chip could include a physiological control, such as urinary creatinine using microfluidics multiplexing [24]. The biomarker panel we propose here is a valuable multi-omics proof-of-concept that might be improved by introducing additional analytes.

Further studies leading to a full clinical trial employing the diagnostic method suggested in this research is required to demonstrate that the platform can deliver an effective POC diagnostic tool for PCa and to determine specificity and robustness against other potential interference including sample-to-sample variations, batch-to-batch discrepancies and stability over time.

The use of multi-omics testing may also have the advantage of characterising the nature of the underlying cancer beyond the simple binary outcomes of current point of care tests. Ultimately, this could result in a test that not only identifies whether cancer is present or not, but one that could distinguish between potentially life-threatening and more benign forms of the disease. Indeed, it is possible that such a test could go further and become a predictive marker, identifying a subgroup of men who might benefit from a specific intervention that prevents progression to a more severe form of the disease.

IV. CONCLUSION

We demonstrate a rapid, accurate and portable CMOS-based multi-omics system capable of simultaneous metabolite and protein quantification. The point-of-care system was used to measure glutamate and aPSA from the same urine sample at the same time in two minutes and is a potential tool to improve the current diagnostic pathways for prostate cancer. The performance of the platform was characterized in buffer and in synthetic urine. The LOD for glutamate and aPSA assays was 0.9 μM and 0.5 ng/ml respectively, making multi-omics POC measurement of metabolites and enzymatically active proteins routinely possible.

This technological breakthrough has the potential to deliver an accurate multi-omics portable device for prostate cancer diagnosis that can potentially reduce the high false-positive rate when used together with a tPSA blood test. Future work will be needed to validate these results in a clinical trial. The platform is suitable for accommodating two independent optical assays therefore the chemistry used can be changed to measure different analytes. The findings of this work are beneficial for applications beyond the immediate clinical test case of PCA.

ACKNOWLEDGMENT

The research was supported by UKRI grants EP/T00097X and EP/K021966.

REFERENCES

- [1] S. Chakraborty, M. I. Hosen, M. Ahmed, and H. U. Shekhar, "Onco-Multi-OMICS Approach: A New Frontier in Cancer Research," *Biomed Research International*, vol. 2018, 2018, doi: 10.1155/2018/9836256.
- [2] Magdalena Stobiecka, Katarzyna Ratajczak, Sławomir Jakiela. "Toward early cancer detection: Focus on biosensing systems and biosensors for an anti-apoptotic protein survivin and survivin mRNA". *Biosensors and Bioelectronics*, Volume 137, 2019, Pages 58-71, ISSN 0956-5663, <https://doi.org/10.1016/j.bios.2019.04.060>.
- [3] E. Zhang et al., "An overview of advances in multi-omics analysis in prostate cancer," *Life Science*, vol. 260, p. 118376, Nov. 2020, doi: 10.1016/J.LFS.2020.118376.
- [4] G. Rodrigues et al., "Pre-treatment risk stratification of prostate cancer patients: A critical review," *Journal of the Canadian Urological Association*, vol. 6, no. 2. Canadian Medical Association, pp. 121–127, 2012, doi: 10.5489/cuaj.11085.
- [5] Ferro, Matteo, et al. "Prostate Health Index (Phi) and Prostate Cancer Antigen 3 (PCA3) significantly improve prostate cancer detection at initial biopsy in a total PSA range of 2–10 ng/ml." *PloS one* 8.7 (2013): e67687.
- [6] A. W. Roddam et al., "Use of prostate-specific antigen (PSA) isoforms for the detection of prostate cancer in men with a PSA level of 2-10 ng/ml: systematic review and meta-analysis," *European Urology*, vol. 48, no. 3, pp. 386–399, 2005, doi: 10.1016/J.EURURO.2005.04.015.
- [7] T. Feng, D. Feng, W. Shi, X. Li, and H. Ma, "A graphene oxide - peptide fluorescence sensor for proteolytically active prostate-specific antigen," *Molecular Biosystems*, vol. 8, no. 5, pp. 1441–1445, Apr. 2012, doi: 10.1039/C2MB05379A.
- [8] M. J. Ahrens, P. A. Bertin, E. F. Vonesh, T. J. Meade, W. J. Catalona, and D. Georganopoulou, "PSA enzymatic activity: A new biomarker for assessing prostate cancer aggressiveness," *Prostate*, vol. 73, no. 16, pp. 1731–1737, Dec. 2013, doi: 10.1002/PROS.22714.
- [9] S. A. Williams, C. A. Jelinek, I. Litvinov, R. J. Cotter, J. T. Isaacs, and S. R. Denmeade, "Enzymatically active prostate-specific antigen promotes growth of human prostate cancers," *Prostate*, vol. 71, no. 15, pp. 1595–1607, Nov. 2011, doi: 10.1002/PROS.21375.
- [10] V. F. Annese et al., "A monolithic single-chip point-of-care platform for metabolomic prostate cancer detection," *Microsystems and Nanoengineering*, vol. 7, no. 1, p. 21, Dec. 2021, doi: 10.1038/s41378-021-00243-4.
- [11] Shen, L. Yan, S. Liu, C. B. Ambrosone, and H. Zhao, "Plasma metabolomic profiles in breast cancer patients and healthy controls: By race and tumor receptor subtypes," *Translational oncology*, vol. 6, no. 6, pp. 757–765, 2013, doi: 10.1593/tlo.13619.
- [12] T. Zhang et al., "Discrimination between malignant and benign ovarian tumors by plasma metabolomic profiling using ultra performance liquid chromatography/mass spectrometry," *Clinica Chimica Acta*, vol. 413, no. 9–10, pp. 861–868, May 2012, doi: 10.1016/j.cca.2012.01.026.
- [13] P. Józwiak, E. Forma, M. Bryś, and A. Krześlak, "O-GlcNAcylation and metabolic reprogramming in cancer," *Frontiers in Endocrinology*, vol. 5, no. SEP. Frontiers Media S.A., 2014, doi: 10.3389/fendo.2014.00145.
- [14] B. Lee et al., "Integrated RnA and metabolite profiling of urine liquid biopsies for prostate cancer biomarker discovery," *Scientific Reports*, 2020, doi: 10.1038/s41598-020-60616-z.
- [15] I. Amelio et al., "Liquid biopsies and cancer omics," *Cell Death Discovery*, vol. 6, no. 1, pp. 1–8, Nov. 2020, doi: 10.1038/s41420-020-00373-0.
- [16] G. J. Tsongalis et al., "Routine use of the Ion Torrent AmpliSeq™ Cancer Hotspot Panel for identification of clinically actionable somatic mutations," *Clinical Chemistry and Laboratory Medicine*, vol. 52, no. 5, pp. 707–714, May 2014.
- [17] H. B. Grossman et al., "Detection of Bladder Cancer Using a Point-of-Care Proteomic Assay," *JAMA*, vol. 293, no. 7, pp. 810–816, Feb. 2005, doi: 10.1001/JAMA.293.7.810.
- [18] Katarzyna Ratajczak, Magdalena Stobiecka. "High-performance modified cellulose paper-based biosensors for medical diagnostics and early cancer screening: A concise review". *Carbohydrate Polymers*, Volume 229, 2020, 115463, ISSN 0144-8617, <https://doi.org/10.1016/j.carbpol.2019.115463>.
- [19] S. B. Patil, V. F. Annese, and D. R. S. Cumming, "Commercial Aspects of Biosensors for Diagnostics and Environmental Monitoring," in *Advances in Nanosensors for Biological and Environmental Analysis*, Elsevier, 2019, pp. 133–142.
- [20] M. A. Al-Rawhani et al., "Multimodal Integrated Sensor Platform for Rapid Biomarker Detection," *IEEE Transactions of Biomedical Engineering*, vol. 67, no. 2, 2020, doi: 10.1109/TBME.2019.2919192.
- [21] V. F. Annese et al., "The Multicorder: A Handheld Multimodal Metabolomics-on-CMOS Sensing Platform," *IEEE 8th International Workshop on Advances in Sensors and Interfaces (IWASI)*. IEEE, 2019. doi: 10.1109/IWASI.2019.8791347.
- [22] "Recombinant Human Kallikrein 3/PSA Protein, CF (1344-SE) | Bio-Techne." (accessed Nov. 17, 2021).
- [23] C. Accarino et al., "Noise characteristics with CMOS sensor array scaling," *Measurement*, vol. 152, Feb. 2020, doi: 10.1016/j.measurement.2019.107325.
- [24] Annese, V.F., et al. "Micromolar Metabolite Measurement in an Electronically Multiplexed Format." *IEEE Transactions on Biomedical Engineering* (2022). doi: 10.1109/TBME.2022.3147855
- [25] Schultz, Jessica, et al. "Glutamate sensing in biofluids: Recent advances and research challenges of electrochemical sensors." *Analyst* 145.2 (2020): 321-347.
- [26] Jones, Alan Wayne. "Lack of association between urinary creatinine and ethanol concentrations and urine/blood ratio of ethanol in two successive voids from drinking drivers." *Journal of analytical toxicology* 22.3 (1998): 184-190.
- [27] S. Bolduc, et al., "Urinary PSA: A potential useful marker when serum PSA is between 2.5 ng/ml and 10 ng/ml," *Canadian Urological Association Journal*, vol. 1, no. 4, pp. 377–381, 2007, doi: 10.5489/cuaj.444
- [28] Kozue Shibata, Jun-ichi Kajihara, Kazuo Kato, Kazuyuki Hirano. Purification and characterization of prostate specific antigen from human urine. *Biochimica et Biophysica Acta (BBA) - General Subjects*. Volume 1336, Issue 3, 1997, Pages 425-433.
- [29] Chan, Kit Man, et al. "Prostate cancer detection: a systematic review of urinary biosensors." *Prostate Cancer and Prostatic Diseases* (2022): 1-8.
- [30] Schultz, Jessica, et al. "Glutamate sensing in biofluids: Recent advances and research challenges of electrochemical sensors." *Analyst* 145, no. 2 (2020): 321-347.
- [31] J. Leinonen, "Immunoassay for Enzymatically Active Prostate-Specific Antigen," *Clinical chemistry*, vol. 129, pp. 125–129, 2004, doi: 10.1373/clinchem.2003.026146.
- [32] P. Niemelä, et al. "Sensitive and Specific Enzymatic Assay for the Determination of Precursor Forms of Prostate-specific Antigen after an Activation Step," *Clinical Chemistry*, vol. 48, no. 8, pp. 1257–1264, Aug. 2002, doi: 10.1093/CLINCHEM/48.8.1257.